BLACK BOX METHODOLOGY FOR THE CHARACTERIZATION OF SAMPLE RATE CONVERSION SYSTEMS

Stéphan Tassart
ST-Ericsson, STS/AEP/CPP
Paris, France
stephan.tassart@stericsson.com

ABSTRACT

Digital systems dedicated to audio and speech processing usually require sample rate conversion units in order to adapt the sample rate from different signal flows: for instance 8 and 16 kHz for speech, 32 kHz for the broadcast rate, 44.1 kHz for CDs and 48 kHz for studio work. The designer chooses the sample rate conversion (SRC) technology based on objective criteria, such as figures of complexity, development or integration cycle and of course performance characterization. For linear time-invariant (LTI) systems, the transfer function contains most information necessary for the system characterization. However, being not LTI, the SRC characterization also requires aliasing characterization. When the system under study is available only through input excitations and output observations (i.e. in black box conditions), aliasing characterization obtained for instance through distortion measurements is difficult to evaluate properly. Furthermore, aliasing measurements can be messed up with weakly nonlinear artifacts, such as those due to internal rounding errors. Consider now the fractional SRC system as a linear periodically time-varying (LPTV) system whose characteristics describe simultaneously the aliasing and the in-band (so-called *linear*) behaviour from the SRC. An interesting and new compound system made of multiple instances of the same SRC system builds a LTI system. The linear features from this compound system fully characterizes the SRC (i.e. its linear and aliasing rejection behaviour) whereas weakly nonlinear features obtained from distortion measurements are only due to internal rounding errors. The SRC system can be analyzed in a black box condition, either in batch processing or real-time processing. Examples illustrate the capability of the method to fully recover characteristics from a multistage SRC system and to separate quantization effect and rounding noise in actual SRC implementations.

1. INTRODUCTION

Evaluating a digital fractional SRC system with tools designed for the evaluation of analog-to-digital convertors (ADC) is an attractive solution. For instance, the instant power measured at the output of the system excited by a swept-sine would assess the *linear* performance of the system whereas a distortion measurement would evaluate the performance of the aliasing rejection [1].

However aliasing effects are a linear effect from a polyphase system [2]. Linear multirate (MRS) [3] and linear periodically time-varying (LPTV) [4, 5] contexts are better suited for discussing fractional SRC systems. The SRC system can be equally represented by a lowpass filter H whose polyphase components form the time varying impulse response of the system. The ideal SRC is fully characterized by the conversion ratio R/P and its lowpass filter H, in particular:

- its passband characteristics (responsable for the resampled signal coloration),
- its stopband characteristics (responsable for the attenuantion of the aliased and mirrored spectral images),
- the *don't care* bandwidth (which defines the bandwidth limitations for incoming signals).

This ideal SRC model is exposed in Section 2. Finite word-length representation causes internal rounding errors and undesired deviations from the ideal model. The method presented in this paper aims at separating the impact of rounding errors from the ideal characteristics in a black box methodology condition. The developments from this paper are limited to the single input single output (SISO) case. The interest follows:

- to provide a common framework for comparing the performances of different SRC algorithms,
- to assess the performances of proprietary SRC algorithms where internals are not available,
- to assess the global performance of complicated multi-stage SRC algorithms.

Section 3 details a compound system based on multiple instances of the SRC system that is LTI. The merits of this LTI compound system for the characterization of sample rate conversion system are discussed in section 3.2. This characterization method is compared to the bispectrum method, used in [6, 7, 2, 8, 9] in order to assess the performances of LPTV systems. Finally, section 4 shows on different examples how traditional black box LTI characterization methods can be used in order to assess the performances of a SRC system.

2. IDEAL MODELS AND NOTATIONS

2.1. Decimation, Expansion and SRC

The building blocks for multirate systems are the delay operator, the decimation operator and the expansion operator [3]. Consider the following real (or complex) scalar signals: x, y, u and v. The expansion operator $\uparrow R$ associates u to x (see Fig. 1) in an operation sometimes refered as *upsampling*:

$$\forall n \in \mathbb{Z}, \quad u(n) = \begin{cases} x\left(\frac{n}{R}\right) & \text{if } n = kR \\ 0 & \text{else.} \end{cases} \tag{1}$$

The decimation operator $\downarrow P$ associates y to v (see Fig. 2) in an operation sometimes refered as *downsampling*:

$$\forall n \in \mathbb{Z}, \quad y(n) = v(nP). \tag{2}$$

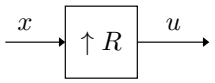

Figure 1: R-fold expansion operator model.

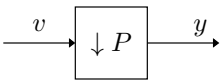

Figure 2: P-fold decimation operator model

The previous definitions respectively for expansion and decimation can be recast in the z-transform domain. The result of the R-fold expansion (see Fig. 1 and equation (1)) verifies in the z-domain:

$$U(z) = X(z^R). \tag{3}$$

The signal y obtained as the P-fold decimation from the signal v (see Fig. 2 and equation (2)) verifies in the z-domain, with ω_P being a P^{th} root of unity:

$$Y(z^P) = \frac{1}{P}\sum_{m=0}^{P-1} V(\omega_P^m z). \tag{4}$$

The multirate system shown in Fig. 3 can be used as an ideal model for a sample rate convertor with a fractional ratio $\times R/P$ as in [5], with R and P chosen coprime. This multirate system consists of a R-fold expansion, a LTI system H refered to as the kernel of the multirate system and a P-fold decimation. The signal v is the result of the filtering of u, i.e. $v(z) = H(z)\cdot u(z)$. Thus, from Eq. (3) and (4), one obtains the modulation equation for the ideal $\times R/P$ sample rate conversion system:

$$Y(z^P) = \frac{1}{P}\sum_{m=0}^{P-1} H(\omega_P^m z)\cdot X(\omega_P^{Rm} z^R). \tag{5}$$

2.2. LPTV systems

A discrete-time linear system is defined as (L_2, L_1)-LPTV if a shift of the input by L_1 samples results in a shift of the output by L_2 samples, for any input signal [2]. Given this definition, the ideal $\times R/P$ sample rate conversion system appears as a (P, R)-LPTV system. Reciprocally, any (P, R)-LPTV system with R and P chosen as two relatively prime integers verifies equation (5) and can be characterized by a kernel H.

2.3. Polyphase type-1 decomposition

The R-polyphase type-1 components[1], $x_{\frac{k}{R}}$, are associated to a signal x in such a way that interleaving those components regenerates the original signal x. In the z-domain, it results:

$$X(z) = \sum_{l=0}^{R-1} z^{-l} X_{\frac{l}{R}}(z^R). \tag{6}$$

[1]Polyphase type-2, type-3 and type-4 are alternate definitions for the polyphase decomposition, cf. [2].

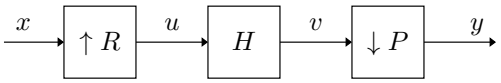

Figure 3: $\times R/P$ sample rate conversion model.

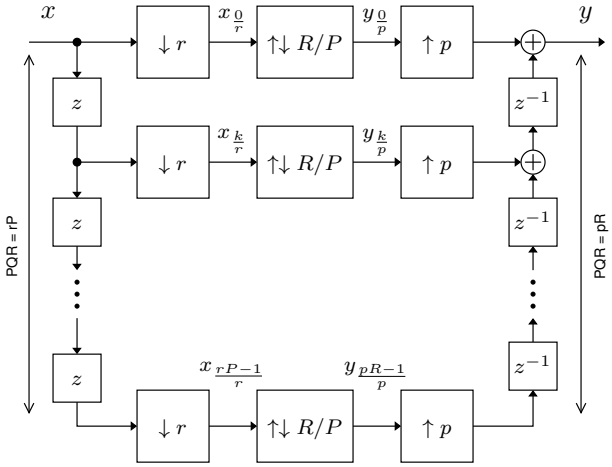

Figure 4: LTI context for a fractional resampler.

This relationship can be inverted [3] and for any k:

$$\forall k \in \mathbb{Z}, \quad X_{\frac{k}{R}}(z^R) = \frac{z^k}{R}\sum_{n=0}^{R-1} \omega_R^{nk} X(\omega_R^n z). \tag{7}$$

3. LTI CONTEXT FOR SRC SYSTEM

3.1. Principles

Consider the compound system described on Fig. 4 where the boxes $\uparrow\downarrow R/P$ represent the whole system given in Fig. 3. Consider Q a positive integer and r and p such as:

$$r = RQ, \quad p = PQ, \quad R/P = r/p.$$

The input signal x is considered as the combination of PQR interleaved channels $x_{\frac{k}{r}}$. The SRC operator $\times R/P$ is applied separately on every channel. The resulting $y_{\frac{k}{p}}$ are interleaved and form a new signal y. The left (resp. right) part of the diagram is related to the QR-polyphase analysis network (resp. PQ-polyphase synthesis network) in [7]. Note that this compound system is not causal because of the usage of the advance operator z. The following result applies:

Theorem 1. *The compound system described in Fig. 4 where the ideal $\times R/P$ sample rate conversion system defined by $H(z)$, the z-transform from its kernel, is applied on PQR channels, and which input x (resp. output y) is obtained by interleaving every channel $x_{\frac{k}{r}}$ (resp. $y_{\frac{k}{p}}$), is LTI.*

Furthermore, y is obtained by filtering x through the expanded kernel of the sample rate conversion system:

$$Y(z) = H(z^Q)\cdot X(z).$$

An important aspect for the proof given in the appendix is the constraint that P and R are relatively prime. In the case of a SRC system, it is always possible to chose P and R relatively prime since only the ratio R/P matters. However, the result from Theorem 1 can not apply to any (L_1, L_2)-LPTV system.

3.2. Discussion

The compound system from Fig. 4 with $Q = 1$ provides a simple methodology for assessing the performance of a SRC system. The kernel H of the SRC system is supposed to have a finite impulse response (FIR) of length L. The typical filter bandwidth is about π/R radians and the typical filter length L is about several times R (depending of the stiffness of the lowpass filter)

- Choose one test vector x from a set of possibly several test vectors.
- De-interleave the test vector x and form the PR channel test vectors $x_{\frac{k}{R}}$. Zero padding can prove to be useful in order to force the SRC system to process the signal until it has returned at rest to a steady-state.
- Apply the SRC system to each different channel vector and obtain the response channel vector $y_{\frac{k}{P}}$. The system under study being supposed to be FIR, the response channel vectors return to 0 after a maximum of $\lceil L/R \rceil$ input zero-padding samples.
- Interleave the PR response channel vectors $y_{\frac{k}{P}}$ and form the response vector y.
- Store the response vector y and repeat the process for every available test vector x.

In short, the SRC system is fed with signals in different phase situations obtained by deinterleaving a given test vector x and the output vectors are interleaved together. The analysis of the SRC system proceeds as if the test vectors x were processed by a regular LTI system. There are different subcases of interest for the test vectors.

Periodic signals are one type of interesting test vectors [7]. Once steady state is achieved (i.e after L samples on the test vector), a single output period is extracted, stored and analyzed. Note that if $N = nPR$, the channel input vectors (resp. channel response vectors) from the compound system are nP-periodic (resp. nR-periodic). Yin and Mehr in [10] use nP-periodic channel input vectors in order to excite and to identify the (R, R)-LPTV system. Transposed to the context of characterizing a SRC system, this identification method implicitly turns into a least-square FIR identification method knowing one period from x and observing one period from y. Compared to these identification methods [7, 10], the LTI approach relaxes the constraints on N which is not a necessary multiple of PR.

The impulse response is another type of interesting test vector. In such case, the impulse response $h(n)$ of the kernel H is directly available in y. When $x(n) = \delta_n$, only remains $X_{\frac{mR}{R}} = z^m$ for $m \in [0, P)$; any other contribution being pure zero:

$$H(z) = Y(z) = \sum_{m=0}^{P-1} z^{-mR} Y_{\frac{mR}{P}}(z^P)$$

$$\forall m \in [0, P) \quad h(nP + mR) = y_{\frac{mR}{P}}(n)$$

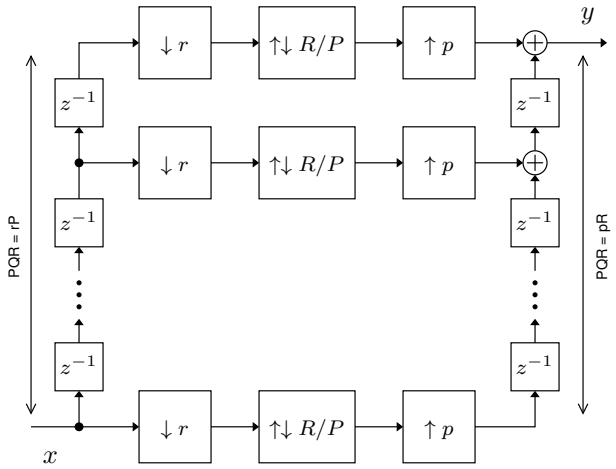

Figure 5: causal LTI context for a fractional resampler.

where n varies in the support from $y_{\frac{mR}{P}}$. The method is indeed valuable and cheap (P channel vectors to process instead of PR) for characterizing an ideal SRC system but it misses the effects from internal rounding errors.

In order to cover those effects, we assume that with orthogonal input signals (obtained for instance by random phase shifting as in [7]), rounding errors average to zero. Distortion observed on the compound system is exclusively due to rounding errors: this can be observed for instance by feeding a full-scale sine in the compound LTI system. Alternatively, the method developped in [11] for measuring the performance of weakly nonlinear system can be used.

Note that the method requires the exact knowledge of the resampling ratio $\times R/P$. A separate adhoc method may be necessary in order to estimate this ratio if it is not explicitly given.

Note also that for complex resampling ratios, such as those encountered for resampling 44.1 kHz audio streams at 48 kHz, the amount of channels becomes large: for $R = 160$ and $P = 147$, we need to process $PR = 23520$ input channel test vectors. A script automating the processing and the storage of each of those PR audio files is needed.

3.3. Causal System

The LTI compound system as described in Fig. 4 is obviously not causal. In the previous discussion, non-causality was not an issue because we assumed that the analysis proceeded in batch processing. Causality may be required for real-time applications. In such case, we can use the type-4 polypase decomposition instead and obtain a causal LTI context for the analysis of a SRC in Fig. 5. The transfer function of the causal LTI compound system becomes:

$$Y(z) = z^{-PQR+1} H(z^Q) \cdot X(z).$$

3.4. Bispectrum analysis

The bispectrum (or bifrequency system function) of a LPTV system is a bivariate function $H(e^{j\omega_1}, e^{j\omega_2})$ that associates the spectrum $Y\left(e^{j\omega_2}\right)$ of the input signal to the spectrum $X\left(e^{j\omega_1}\right)$ of the

output signal (cf. [7]):

$$\forall \omega_2 \in \mathbb{R},\ Y\left(e^{j\omega_2}\right) = \int_{-\pi}^{+\pi} H\left(e^{j\omega_1}, e^{j\omega_2}\right) X\left(e^{j\omega_1}\right)\, \mathrm{d}\omega_1. \quad (8)$$

Theorem 2. *The bispectrum $H(e^{j\omega_1}, e^{j\omega_2})$ of the ideal $\times R/P$ sample rate conversion system consists of Dirac lines deriving from $H(e^{j\omega})$, the transfer function of its kernel:*

$$H\left(e^{j\omega_1}, e^{j\omega_2}\right) = \frac{1}{P} \sum_{m=0}^{P-1} H\left(e^{j\frac{\omega_1}{R}}\right) \delta\left(P\omega_1 - R\left(\omega_2 + 2m\pi\right)\right)$$

where δ corresponds to the Dirac distribution.

Due to the fact that R and P are relatively prime, the different Dirac lines exhibited by the bispectrum reduce to one single Dirac line shaped by the transfer function of the SRC kernel and repeated along the quadrants.

Therefore the spectrum analysis of the LTI compound system compares to the bispectrum analysis of the LPTV system as in [6]. Kernel spectrum and bispectrum can both be retreived in black box conditions. It is however our opinion that the LTI approach obtained from the compound system from Fig. 4 is more flexible than the bispectrum approach: constraints about input signal are relaxed and analysis methods are more straighforward to use because directly derived from traditional methods.

4. EXAMPLES

4.1. Upsampler $\times 3$

Figures 6 and 7 illustrate how the kernel transfer function from two x3 in-house upsampler algorithms can be revealed with the LTI methodology. The upsampling algorithms under study were provided as binary executable files that process soundfiles in double precision floating point arithmetic. The soundfiles are stored in single precision floating point (i.e. 24-bit mantissa). Both algorithms proceed in two stages, including first an upsampling block (resp. $\times 128$ and $\times 4$) and a decimating block obtained by polynomial interpolation (resp. linear interpolation and quadric interpolation) as in [12]. The actual upsampler kernel is difficult to evaluate in a formal way due to the presence of the polynomial interpolation block.

In order to reveal the upsampler kernel transfer function, two complementary test vectors, $x^{(1)}$ and $x^{(2)}$ are generated. The first test vector $x^{(1)}$ is generated as the impulse response of a low-order lowpass filter (with a cutoff frequency approximatively set to $\pi/2$). The second test vector $x^{(2)}$ was generated by the modulation of $x^{(1)}$ at the Nyquist frequency. The tranfer function $H(e^{j\omega})$ is obtained as a weighted sum of the ratio $Y(e^{j\omega})/X(e^{j\omega})$ for each available test vector:

$$H\left(e^{j\omega}\right) = \frac{1}{\sum_i W^{(i)}(\omega)} \times \sum_i W^{(i)}(\omega) \frac{Y^{(i)}\left(e^{j\omega}\right)}{X^{(i)}\left(e^{j\omega}\right)}.$$

In this example, the weight $W^{(i)}(\omega)$ was set to $|X^{(i)}(e^{j\omega})|^2$. Fig. 6 demonstrates that in-band ripples behave accordingly to the specifications, resp. ± 0.002 dB and ± 0.01 dB. Fig. 7 demonstrates that the alias rejection performance matches the -94 dB specification only for the second algorithm. Examination of both figures demonstrates that the *don't care* bandwidth matches the specified band $[0.9\pi, 1.1\pi]/3$.

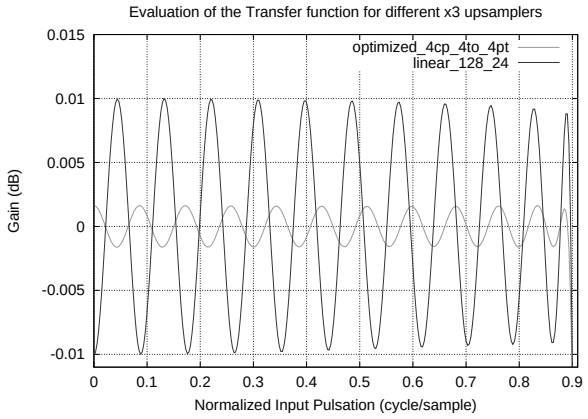

Figure 6: Estimated upsampler $\times 3$ transfer function, passband details.

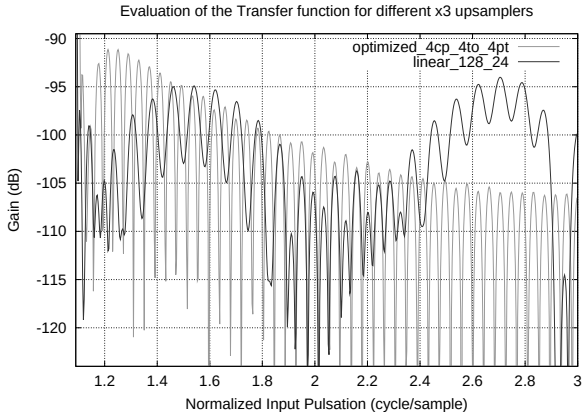

Figure 7: Estimated upsampler $\times 3$ transfer function, stopband details.

4.2. Resampler $\times 3/2$

Figures 8 and 9 illustrate how different types of arithmetic impact measurements obtained from the LTI methodology. The SRC system under study is an in-house one-stage $\times 3/2$ SRC implementation available respectively in double precision floating point arithmetic, in 24-bit fixed-point arithmetic and in 16-bit fixed-point arithmetic. The algorithms were provided in an executable format.

Fig. 8, obtained with the set of test vectors from section 4.1, illustrates the impact of the filter coefficients quantization. The 24-bit coefficient quantization provides an accuracy compatible with the stopband specification whereas the 16-bit quantization does not.

Fig. 9 demonstrates the impact of internal rounding errors on a pure sine located at $\pi/8$. The noise floor due to the storage format is about -186 dB. The harmonic distortion observed for the floating-point version of the algorithm serves as a reference assessing the impact from both the double-precision floating-point internal rounding errors and the quantization due to the file format storage. This reference is about -160 dB. The differences between the reference blue line and the dotted red (resp. dotted

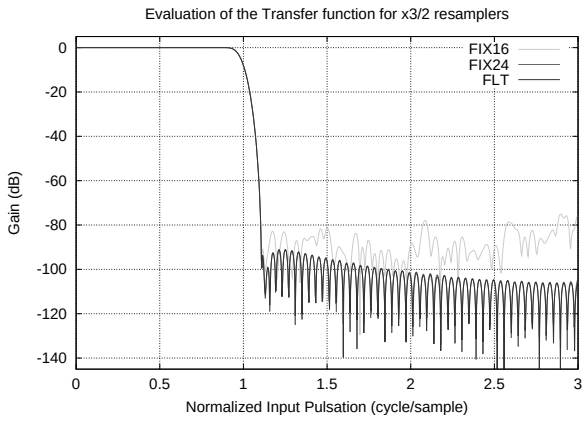

Figure 8: Transfer function of a $\times 3/2$ resampler implemented with different types of arithmetic.

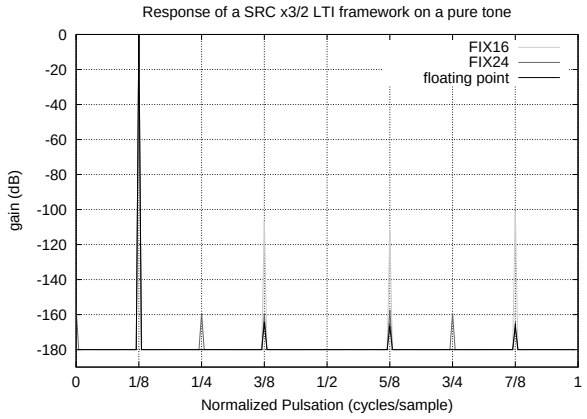

Figure 9: Impact of the internal rounding errors evaluated on a full-scale sine for a $\times 3/2$ resampler implemented with different types of arithmetic.

green) curve on Fig. 9 are only due to rounding errors in the 24-bit (resp. 16-bit) fixed-point arithmetic. In the implemented algorithm, the impact of the rounding errors in the 24-bit fixed-point arithmetic seems neglectable with regard to the alias level. In the 16-bit arithmetic, the impact of internal rounding error is more sensible but still limited with regard to the actual performance of the alias rejection. Interestingly, only odd harmonics are generated in 16-bit fixed-point arithmetic. Note that the impact of the rounding errors is quite limited in this example because the SRC processing is single stage and the rounding error happens only once per output sample without propagation when the result of the double precision accumulation is cast back into single precision. A more complex situation is expected when the SRC algorithm involves multiple stages or polynomial interpolation.

5. CONCLUSION

In this paper, we have discussed the merits of a compound system made of several instances of a sample rate conversion systems. This compound system is LTI and its transfer function, $H(z^Q)$, is directly related to the transfer function of the SRC kernel. Regular identification and characterization methods designed for LTI systems can be applied on this system in order to reveal the linear characteristics responsable for both the in-band and the aliasing behaviour and the weakly nonlinear characteristics due to the propagation of rounding errors. This LTI context simplifies the analysis method proposed in [7] when the periods from the LPTV systems are relatively prime.

6. REFERENCES

[1] Walt Kester, Ed., *The Data Conversion Handbook*, Elvesier, 2005.

[2] R.L. Reng, "Polyphase and modulation descriptions of multirate systems - A systematic approach," in *Proc. Int. Conf. DSP*, Limassol, Cyprus, June 1995, pp. 212–217.

[3] P. P. Vaidyanathan, *Multirate Systems and Filter Banks*, Prentice Hall, 1993.

[4] R. Meyer. and C. Burrus, "A unified analysis of multirate and periodically time-varying digital filters," *Circuits and Systems, IEEE Transactions on*, vol. 22, no. 3, pp. 162–168, Mar. 1975.

[5] A.S. Mehr and T. Chen, "Representations of linear periodically time-varying and multirate systems," *Signal Processing, IEEE Transactions on*, vol. 50, no. 9, pp. 2221–2229, Sept. 2002.

[6] R.L. Reng and H.W. Schüßler, "Measurement of aliasing distortions and quantization noise in multirate systems," in *Circuits and Systems, 1992. ISCAS '92. Proceedings., 1992 IEEE International Symposium on*, May 1992, vol. 5, pp. 2328–2331.

[7] F.A. Heinle and H.W. Schüßler, "An enhanced method for measuring the performance of multirate systems," in *In Proc. Int. Conf. on Digital Signal Processing, Limassol*, 1995, pp. 182–187.

[8] F. Heinle, R. Reng, and G. Runze, "Symbolic analysis of multirate systems," *Maple Technical Newsletter*, vol. 3, no. 1, 1996, Special Issue featuring Engineering Applications.

[9] F.A. Heinle and H.W. Schüßler, "Measuring the performance of implemented multirate systems," in *Acoustics, Speech, and Signal Processing, 1996. ICASSP-96. Conference Proceedings., 1996 IEEE International Conference on*, May 1996, vol. 5, pp. 2754–2757.

[10] W. Yin and A.S. Mehr, "Identification of linear periodically time-varying systems using periodic sequences," in *Control Applications, (CCA) Intelligent Control, (ISIC), 2009 IEEE*, July 2009, pp. 1455–1459.

[11] H.W. Schüßler, Y. Dong, and R. Reng, "A new method for measuring the performance of weakly nonlinear systems," in *Acoustics, Speech, and Signal Processing, 1989. ICASSP-89., 1989 International Conference on*, May 1989, vol. 4, pp. 2089–2092.

[12] O. Niemitalo, "Polynomial interpolators for high-quality resampling of oversampled audio," `http://www.student.oulu.fi/~oniemita/dsp/deip.pdf`, Aug. 2001.

A. PROOFS FOR THE THEOREMS

Proof for Theorem 1. Let Q be any positive natural integer. Name r (resp. p) the integer $r = RQ$ (resp. $p = PQ$). The parameters P, R, r and p are associated through the following properties:

$$r = RQ, \quad p = PQ, \quad R/P = r/p, \quad P \wedge R = 1. \tag{9}$$

We use equation (7) in order to describe the signal x as the interleaving from the input channels $x_{\frac{k}{r}}$:

$$\forall k \in \mathbb{Z}, \quad X_{\frac{k}{r}}(z^r) = \frac{z^k}{r} \sum_{n=0}^{r-1} \omega_r^{nk} X(\omega_r^n z).$$

In order to continue the calculous, we introduce intermediary variables. First, let define the composite root $\Omega_{m,n}$ as:

$$\begin{aligned} \forall m \in [0,P), \quad \forall n \in [0,r), \quad \Omega_{m,n} &= \omega_p^m \omega_r^n \\ &= \omega_{PQR}^{mR+nP} \end{aligned}$$

then define the intermediary functions $\chi_l^m(z)$ and $\chi_m(z)$ as:

$$\forall l \in [0,P), \quad \chi_l^m(z) = \sum_{k=0}^{Q-1} z^{-k} X_{\frac{k+lQ}{r}}(\omega_P^{Rm} z^r),$$

$$\begin{aligned} \forall m \in [0,P), \qquad \chi_m(z) &= \frac{1}{P} \sum_{l=0}^{PR-1} z^{-lQ} \chi_l^m(z) \\ &= \frac{1}{P} \sum_{l=0}^{PR-1} \sum_{k=0}^{Q-1} z^{-(k+lQ)} X_{\frac{k+lQ}{r}}(\omega_P^{Rm} z^r). \end{aligned}$$

Notice that $k + lQ$ with $k \in [0,Q)$ and $l \in [0,PR)$ covers the entire range $[0,pR)$. Therefore, the previous sum can be rewritten as:

$$\forall m \in [0,P), \quad \chi_m(z) = \frac{1}{P} \sum_{k=0}^{pR-1} z^{-k} X_{\frac{k}{r}}(\omega_P^{Rm} z^r).$$

Let evaluate $X_{\frac{k+lQ}{r}}(z^r)$ first, $X_{\frac{k+lQ}{r}}(\omega_P^{Rm} z^r)$ then

$$X_{\frac{k+lQ}{r}}(z^r) = \frac{z^{k+lQ}}{r} \sum_{n=0}^{r-1} \omega_r^{n(k+lQ)} X(\omega_r^n z).$$

For the second evaluation, notice $\omega_{rP}^{Rm} = \omega_{Rp}^{Rm} = \omega_p^m$ and therefore:

$$\begin{aligned} X_{\frac{k+lQ}{r}}(\omega_P^{Rm} z^r) &= X_{\frac{k+lQ}{r}}\left((\omega_p^m z)^r\right) \\ &= \frac{\left(\omega_p^m z\right)^{k+lQ}}{r} \sum_{n=0}^{r-1} \omega_r^{n(k+lQ)} X(\omega_p^m \omega_r^n z) \\ &= \frac{z^{k+lQ}}{r} \sum_{n=0}^{r-1} \Omega_{m,n}^{k+lQ} X(\Omega_{m,n} z). \end{aligned}$$

Now, let evaluate $\chi_l^m(z)$ and finaly $\chi_m(z)$:

$$\begin{aligned} \chi_l^m(z) &= \sum_{k=0}^{Q-1} z^{-k} X_{\frac{k+lQ}{r}}(\omega_P^{Rm} z^r) \\ &= \frac{z^{lQ}}{r} \sum_{k=0}^{Q-1} \sum_{n=0}^{r-1} \Omega_{m,n}^{k+lQ} X(\Omega_{m,n} z), \end{aligned}$$

$$\begin{aligned} \chi_m(z) &= \frac{1}{P} \sum_{l=0}^{PR-1} z^{-lQ} \chi_l^m(z) \\ &= \frac{1}{rP} \sum_{l=0}^{PR-1} \sum_{k=0}^{Q-1} \sum_{n=0}^{r-1} \Omega_{m,n}^{k+lQ} X(\Omega_{m,n} z) \\ &= \frac{1}{PQR} \sum_{k=0}^{PQR-1} \sum_{n=0}^{r-1} \Omega_{m,n}^{k} X(\Omega_{m,n} z). \end{aligned}$$

The response channels signal $y_{\frac{k}{p}}$ results from the application of the fractional SRC to $x_{\frac{k}{r}}$. Apply equation (5):

$$Y_{\frac{k}{p}}(z^P) = \frac{1}{P} \sum_{m=0}^{P-1} H(\omega_P^m z) \cdot X_{\frac{k}{r}}(\omega_P^{Rm} z^R).$$

The signal y is obtained by interleaving every channel $y_{\frac{k}{p}}$:

$$\begin{aligned} Y(z) &= \sum_{k=0}^{pR-1} z^{-k} Y_{\frac{k}{p}}(z^p) \\ &= \sum_{k=0}^{pR-1} z^{-k} Y_{\frac{k}{p}}(z^{PQ}) \\ &= \frac{1}{P} \sum_{k=0}^{pR-1} z^{-k} \sum_{m=0}^{P-1} H(\omega_P^m z^Q) \cdot X_{\frac{k}{r}}(\omega_P^{Rm} z^r) \\ &= \frac{1}{P} \sum_{m=0}^{P-1} H(\omega_P^m z^Q) \sum_{k=0}^{pR-1} z^{-k} X_{\frac{k}{r}}(\omega_P^{Rm} z^r) \\ &= \sum_{m=0}^{P-1} H(\omega_P^m z^Q) \chi_m(z). \end{aligned}$$

This concludes the evaluation of $Y(z)$ in term of the modulation components $X(\Omega_{m,n} z)$:

$$Y(z) = \frac{1}{PQR} \sum_{m=0}^{P-1} \sum_{k=0}^{pR-1} \sum_{n=0}^{r-1} H(\omega_P^m z^Q) \Omega_{m,n}^k X(\Omega_{m,n} z).$$

Since P and R are coprime, $mR + nP \mod (PQR)$ covers exactly the range $[0,PQR)$ when $m \in [0,P)$ and $n \in [0,RQ)$. Let apply the Chinese remainder theorem: the double sum in m and n can be replaced by a simple sum in i, with $m = i \times \bar{R}$, labelling $\bar{R}$ the multiplicative inverse from R in the ring $\mathbb{Z}/P\mathbb{Z}$:

$$\begin{aligned} Y(z) &= \frac{1}{PQR} \sum_{i=0}^{PQR-1} \sum_{k=0}^{pR-1} H(\omega_P^{i\bar{R}} z^Q) \omega_{PQR}^{ik} X(\omega_{PQR}^i z) \\ &= \frac{1}{PQR} \sum_{i=0}^{PQR-1} \sum_{k=0}^{PQR-1} \omega_{PQR}^{ik} H(\omega_{PQR}^{iQ} z^Q) X(\omega_{PQR}^i z). \end{aligned}$$

Since ω_{PQR} is a root of the unity, we have:

$$\sum_{k=0}^{PQR-1} \omega_{PQR}^{ik} = PQR \sum_n \delta_{i-nPQR}.$$

Every modulation component vanishes from $Y(z)$ and only remains:

$$Y(z) = H(z^Q) \cdot X(z). \tag{10}$$

This concludes the demonstration because the vanishing of every modulation component $X(\omega_{PQR}^i z)$ from $Y(z)$ proves that the system is LTI. □

Proof for Theorem 2. The proof is obtained by substituting the expression of the bispectrum in equation (8). The Dirac lines, located at $\omega_1 = R/P\,(\omega_2 + 2m\pi)$, simplify the integral expression:

$$Y\left(e^{j\omega_2}\right) = \frac{1}{P}\sum_{m=0}^{P-1} H\left(e^{j\frac{\omega_2+2m\pi}{P}}\right) X\left(e^{j\frac{R}{P}(\omega_2+2m\pi)}\right).$$

In order to simplify the notation from the previous expression, introduce ω such as $\omega_2 = P\omega$:

$$Y\left(e^{jP\omega}\right) = \frac{1}{P}\sum_{m=0}^{P-1} H\left(e^{j\left(\omega+\frac{2m\pi}{P}\right)}\right) X\left(e^{jR\left(\omega+\frac{2m\pi}{P}\right)}\right).$$

The modulation equation (5) that characterizes the ideal $\times R/P$ SRC system can be recognized here, where z is substituted by $e^{j\omega}$. This concludes the proof by identification of the bifrequency function. □